



Antitumor Effect of Bio-Fabricated Silver Nanoparticles Towards Ehrlich Ascites Carcinoma

Reena Kumari ¹ , Adesh Kumar Saini ² , Anil Kumar Chhillar ³ , Vipin Saini ⁴ ,
Reena V. Saini ^{2,*} 

¹ School of Biotechnology, Faculty of Applied Sciences and Biotechnology, Shoolini University of Biotechnology and Management Sciences, Solan, Himachal Pradesh, 173229, India

² Department of Biotechnology, MMEC, Maharishi Markandeshwar (Deemed to be University), Mullana- Ambala, Haryana, 133207, India

³ Centre of Biotechnology, Maharishi Dayanand University, Rohtak, Haryana, 124001, India

⁴ Maharishi Markandeshwar University, Solan, Himachal Pradesh, 173229, India

* Correspondence: reenavohra10@mmumullana.org; reenavohra10@gmail.com;

Scopus Author ID 35554038200

Received: 29.12.2020; Revised: 19.01.2021; Accepted: 23.01.2021; Published: 31.01.2021

Abstract: The current study aimed to evaluate the *in vitro* and *in vivo* anticancer potential of the silver nanoparticles fabricated with butanol fraction of *Pinus roxburghii* needles (PNb-AgNPs). *In vitro* results revealed significant cytotoxicity of PNb-AgNPs towards Ehrlich Ascites Carcinoma (EAC) cells with an IC₅₀ of 47.02 ± 1.11 µg/ml. Further, morphological changes, Reactive Oxygen Species (ROS) generation, mitochondrial depolarization, and DNA fragmentation elucidated EAC cell death by PNb-AgNPs exposure. The cell cycle analysis displayed an increase in the Sub-G1 population (52%), further confirmed by nuclear fragmentation in EAC cells after PNb-AgNPs treatment. The hemolytic investigation revealed the biocompatible nature of PNb-AgNPs. *In vivo* experiments were performed using the liquid Ehrlich Ascites Carcinoma tumor model, which clearly showed a reduction in tumor growth and body weight following PNb-AgNPs treatment in EAC-bearing mice as compared to untreated controls. Moreover, elevated hematological and biochemical parameters were found to restore to normal range in EAC-bearing mice treated with PNb-AgNPs. Overall, PNb-AgNPs effectively induced apoptotic cell death in EAC cells and exhibited remarkable *in vivo* antitumor potential.

Keywords: *Pinus roxburghii*; silver nanoparticles; Ehrlich Ascites Carcinoma.

© 2021 by the authors. This article is an open-access article distributed under the terms and conditions of the Creative Commons Attribution (CC BY) license (<https://creativecommons.org/licenses/by/4.0/>).

1. Introduction

Cancer is one of the complex, multifaceted diseases with high mortality rates in the world [1]. In 2018 approximately, 9.5 million patients died of cancer, which is expected to increase to 16.3 million by 2040 [2]. It is well known that multiple genetic and environmental factors are responsible for cancer. Knowledge of these factors and tumor microenvironment can provide new targets and approaches for cancer therapy. Despite extensive research and advancements in novel approaches, current treatments are still restricted to conventional therapies (surgery, radiotherapy, chemotherapy) [3]. The chemotherapeutic agents used for cancer treatment cause multiple drug resistance in cancer cells and severe toxicity to healthy cells [4, 5].

Nanomedicine is one of the innovative cancer treatment approaches by facilitating targeted delivery to the tumor site [6, 7]. The unique physicochemical characteristics of metal nanoparticles, such as small size, higher reactivity, high surface to volume ratio, ease of

synthesis, and surface functionalization, provide a new cancer therapeutics scenario. Silver nanoparticles (AgNPs) have become the object of intense research because of their multiple applications in the biomedical area. Several methods have been developed to synthesize noble metal nanoparticles [8]. Biological methods are currently getting the researchers' attention for metal nanoparticle synthesis. They are preferred over physicochemical methods as they are cost-effective, non-toxic, and environment friendly [9, 10]. Plant extracts or bioactive compounds are considered the best for the production of metal nanoparticles. They are appropriate for large-scale biosynthesis of non-toxic nanoparticles quickly with greater applicability and simplicity [11, 12].

Apoptosis, the natural mechanism of programmed cell death induced in cancer cells, is considered a promising approach to anticancer therapy [13]. The unique characteristics of cells undergoing apoptosis are cell shrinkage, chromatin condensation, membrane blebbing, and formation of apoptotic bodies. The extensively studied apoptosis pathways are DNA fragmentation and reactive oxygen species (ROS) formation [14]. Earlier studies have shown that the cytotoxicity mediated through synthesized AgNPs is associated with an enhanced level of cellular reactive oxygen species (ROS), mitochondrial membrane disruption, and DNA fragmentation [15].

In our previous study, AgNPs were fabricated using a butanol fraction of *Pinus roxburghii* needles (PNb-AgNPs). Since the butanol fraction of *P. roxburghii* needles showed higher anticancer potential than other fractions (Methanol, Chloroform, Ethyl acetate, and Aqueous), therefore, butanol fraction was utilized for AgNPs synthesis. The biosynthesized PNb-AgNPs could induce apoptosis in lung adenocarcinomas (A549) and PC-3 Prostate carcinomas [16].

In the present study, the anticancer effect of biosynthesized PNb-AgNPs was investigated against Ehrlich ascites carcinoma (EAC) under both *in vitro* and *in vivo* conditions. EAC cells are murine mammary adenocarcinomas characterized by a high proliferation rate and transplantation potential [17]. EAC cells were derived from mice breast cancer, which were very similar to human tumors and highly sensitive to anticancer drugs [18, 19]. The biocompatibility of PNb-AgNPs was analyzed by the RBC lysis assay. PNb-AgNPs displayed ROS-dependent cell death through apoptosis under *in vitro* conditions, further confirmed by DAPI staining, DNA fragmentation, and an increase in the sub-G1 population. Results displayed the potent anticancer activity of PNb-AgNPs towards EAC cells.

2. Materials and Methods

2.1. Materials.

3-(4,5 -dimethylthiazol-2-yl)-2, 5-diphenyl tetrazolium bromide (MTT), Dulbecco's Modified Eagle's Medium (DMEM), Phosphate Buffer Saline (PBS), Fetal Bovine Serum (FBS), Propidium Iodide (PI), Triton X-100 and 5-Fluorouracil (5-FU) were purchased from Himedia (Mumbai, India). Rhodamine 123 (Rh123) and 2,7- Dichlorofluorescein Diacetate (H₂DCF-DA) were purchased from Sigma Aldrich, and 4',6-Diamidino-2-Phenylindole (DAPI) was procured from Thermo fisher scientific.

2.2. Cell line.

Ehrlich ascites carcinoma cell line was purchased from National Centre for Cell Sciences, Pune, India was maintained in DMEM supplemented with 10% (v/v) FBS and 1%

penicillin/streptomycin solution (10,000 Units/mL penicillin and 10,000 µg/mL streptomycin) in 5% CO₂ at 37 °C.

2.3. Anticancer activity of PNB-AgNPs by MTT assay.

As mentioned above, PNB-AgNPs have been synthesized and characterized earlier [16]. Butanol fraction was used to engineer these nanoparticles. Therefore, butanol fraction was utilized for comparison in both *in vitro* and *in vivo* experiments. The anticancer activity of PNB-AgNPs against EAC cells was evaluated using the MTT assay. EAC cells (1×10⁴ cells/well) were seeded in a 96-well plate and grew overnight. Various concentrations of butanol fraction of *P. roxburghii* and PNB-AgNPs (25, 50, 100, and 200 µg/ml) were added to the cells and incubated for 24 h. Cells alone served as the negative control. After treatment, the cells were washed by PBS solution and then incubated with 20 µl (5mg/ml) of MTT in a fresh medium for 4 h at 37 °C. After incubation, the medium was removed, and 100 µl DMSO was added to solubilize the resultant formazan crystals from the mitochondrial reduction of MTT. The absorbance was determined using a microplate reader (Varioskan LUX, Thermo Scientific) at 570 nm. The percentage of cell death was calculated via the following equation:

$$\% \text{ Cell death} = \frac{\text{OD}_{\text{control}} - \text{OD}_{\text{sample}}}{\text{OD}_{\text{control}}} \times 100$$

Where, OD_{control} represents optical density for untreated cells, and the OD_{sample} represents optical density for sample treated cells.

2.4. Intracellular ROS generation analysis.

EAC cells (5 × 10⁴ cells/ well) were seeded in 6 well-plate and treated with butanol fraction and PNB-AgNPs (200 µg/ ml) for 24 h. After treatment, cells were collected and suspended in PBS with H₂DCF-DA at a final concentration of 20 µM at 37 °C for 20 min. Then, the stained cells were collected and resuspended in PBS. The ROS level was evaluated by measuring the fluorescence intensity using a spectrofluorometer (Varioskan LUX, Thermo Scientific) at 485 nm excitation and 530 nm emission wavelengths [20]. Results were expressed as a fold increase in ROS production compared to that of untreated cells. The experiment was performed in triplicate.

2.5. Mitochondrial membrane potential (MMP).

EAC cells (5 × 10⁴ cells/well) were seeded in a 6 well-plate. After 24 h treatment with butanol fraction and PNB-AgNPs (200 µg/ ml), collected cells were suspended in PBS with 50 µM Rh 123 for 20 min at 37 °C in a humidified chamber. Then, the fluorescence intensity of Rh 123 was examined using Varioskan LUX, Thermo Scientific, spectrophotometer at an excitation wavelength of 507 nm and an emission wavelength of 534 nm [21]. Results were expressed as relative units of fluorescence.

2.6. Cell cycle analysis.

Flow cytometric analysis was done to characterize the effect of PNB-AgNPs on cell cycle distribution using propidium iodide (PI) staining. EAC cells (1×10⁶) were seeded in the 6-well plate, incubated at 37 °C in a humidified atmosphere to allow them to adhere overnight. Cells were then treated with butanol fraction and PNB-AgNPs at a known concentration (200

µg/ml) for 24 h. After 24 h incubation, treated cells were washed twice with ice-cold PBS. The cells were fixed in 70 % ethanol overnight at 4 °C. The cells were then stained with propidium iodide. The cell cycle distribution was determined using a Flow Canto II- flow cytometer at Post Graduate Institute of Medical Education & Research, Chandigarh, India. Doxorubicin and cells alone were used as positive and negative controls, respectively.

2.7. Nuclear morphology analysis.

EAC cells were treated with 200 µg/ml of butanol fraction and PNb-AgNPs for 24 h while doxorubicin was used as a positive control. Cells were washed two times with PBS and fixed in 4% paraformaldehyde for 15 minutes. After washing with PBS, cells were permeabilized with 0.1% Triton-X 100 for 15 min and stained with DAPI in the dark for 20 min. After PBS washing, the nuclear morphology of cells was determined by fluorescence microscopy at 20× magnification (Olympus 1X 51).

2.8. DNA fragmentation by PNb-AgNPs.

EAC cells treated with 200 µg/ml of butanol fraction and PNb-AgNPs for 24 h were harvested and washed. The cells were lysed using lysis buffer (50mM Tris, 20mM EDTA, 0.5% Triton-X 100) for 30 min on ice. The lysates were centrifuged at 11,000 rpm for 20 min, and the supernatant was collected. The supernatant was further incubated with 1% sodium dodecyl sulfate (SDS) and RNase A (0.1mg/ml) for 1 hr at 37 °C, followed by proteinase K treatment for 2 h at 56 °C. After completing both incubation steps, DNA from the supernatant was extracted with phenol:chloroform:isoamyl alcohol (25:24:1 v/v/v) and precipitated with an equal volume of isopropanol at -20 °C overnight. DNA fragments were resolved by 1.8 % agarose gel electrophoresis and visualized with an ultraviolet gel documentation system [22].

2.9. Hemolysis evaluation.

The biocompatible nature of PNb-AgNPs was analyzed by RBC lysis assay of Swiss albino mice RBCs (Approval no., from institutional animal ethical committee IAEC/SU-PHARM/15/02). Blood was collected in K2-EDTA- coated vacutainer tubes, centrifuged at 1500 rpm for 5 min, and plasma was aspirated. The erythrocytes were washed with 150 mM NaCl solution and then resuspended in PBS. The erythrocytes were incubated at 37 °C for one hour with various concentrations (125, 250, 500, 1000 µg/ml) of butanol fraction and PNb-AgNPs. The treated blood cells were again centrifuged for 5 min at 1500 rpm to pellet intact erythrocytes. The absorbance of the supernatants was measured spectrophotometrically at 540 nm. Triton X-100 (10%) and PBS were taken as positive and negative controls, respectively [23].

$$\text{Haemolysis (\%)} = \frac{\text{OD}_{\text{Test sample}} - \text{OD}_{\text{Negative control}}}{\text{OD}_{\text{Positive control}} - \text{OD}_{\text{Negative control}}} \times 100$$

2.10. In vivo anticancer studies via PNb-AgNPs.

Female Swiss albino mice (25-30 g) used for the study were purchased from the National Institute of Pharmaceutical Education and Research, Mohali, India. The animals were maintained on a regular day and night conditions (12 h light: 12 h dark) on pelleted feed and water (ad libitum). The study's animal models and experiments were approved by the Institutional Animal Ethical Committee (IAEC/SU-PHARM/15/02).

2.10.1. Tumor cells.

The EAC cells were maintained *in vivo* by inoculating 2×10^6 cells in the peritoneal cavity (I.P.) of female Swiss albino mice and propagated for 12 to 14 days. Animals were sacrificed to collect the tumor cells and to start the experiment.

2.10.2. Experimental procedure.

The animals were randomly divided into five groups (six animals in each group), which were given the following treatment: Group I (control group) did not receive EAC cells, and all other groups were injected with 2×10^6 EAC cells intraperitoneally. The day of tumor inoculation was considered zero-day, and treatment was started after 48 h of cell inoculation. Group II served as tumor control. Group III mice were treated with butanol fraction (6 mg/kg body wt.), and group IV mice received PNB-AgNPs (2 mg/kg body wt.) for 14 days. The doses were selected based on the IC₅₀ values obtained by *in vitro* studies. Group V (positive control) animals were treated with standard anticancer drug 5-Fluoro Uracil (5- FU, 20 mg/kg body wt.) for 14 days.

2.10.3. Antitumor studies (bodyweight, tumor cell count, and tumor volume).

The body weight of all the experimental animals was measured from day 0 to day 14. On the 15th day, after overnight fasting, mice were sacrificed to collect the ascitic fluid from the peritoneal cavity to evaluate tumor volume and tumor cell count. The inhibition of tumor growth was measured by comparing the number of EAC cells present in the tumor control group (Group II) and treated groups.

2.10.4. Hematology and biochemical analysis.

Blood samples were collected from retro-orbital plexus from experimental animals in EDTA-coated vials. Whole blood was used to estimate hemoglobin content, red blood cells (RBC), and white blood cells (WBC) count. Further, to assess drug-induced hepatotoxicity, the serum was subjected to liver function tests such as aspartate aminotransferase (AST), alanine aminotransferase (ALT), and alkaline phosphatase (ALP).

2.10.5. Histopathological study.

For the histopathological study, liver tissues were preserved in 10 % formalin. The staining of these preserved samples was done by hematoxylin-eosin staining technique for paraffin embedded tissue sections. The histopathological tissue sections of the liver were observed under the microscope and photographed at 100× magnification.

2.11. Statistical analysis.

One-way analysis of variance (ANOVA) evaluated the results' statistical significance using Graph Pad Prism 5.0. A value of $p \leq 0.05$ was considered to indicate a significant difference between the groups. The data were expressed as mean \pm standard error mean (SEM).

3. Results and Discussion

3.1. In vitro cytotoxicity of PNb-AgNPs.

The MTT assay revealed that PNb-AgNPs significantly inhibit EAC cells' growth with an increase in concentration (25 -200 $\mu\text{g/ml}$) (Figure 1a). The IC_{50} values against EAC cells were $47.02 \pm 1.11 \mu\text{g/ml}$ for PNb-AgNPs and $174.01 \pm 1.23 \mu\text{g/ml}$ for the butanol fraction of *P. roxburghii*. The microscopic images (Figure 1b) clearly showed the cytotoxic effect of PNb-AgNPs as compared to butanol fraction and untreated control cells. The enhanced anticancer activity of PNb-AgNPs could be due to the unique physicochemical properties of nanoparticles, such as smaller particle size and enhanced surface volume ratio [24].

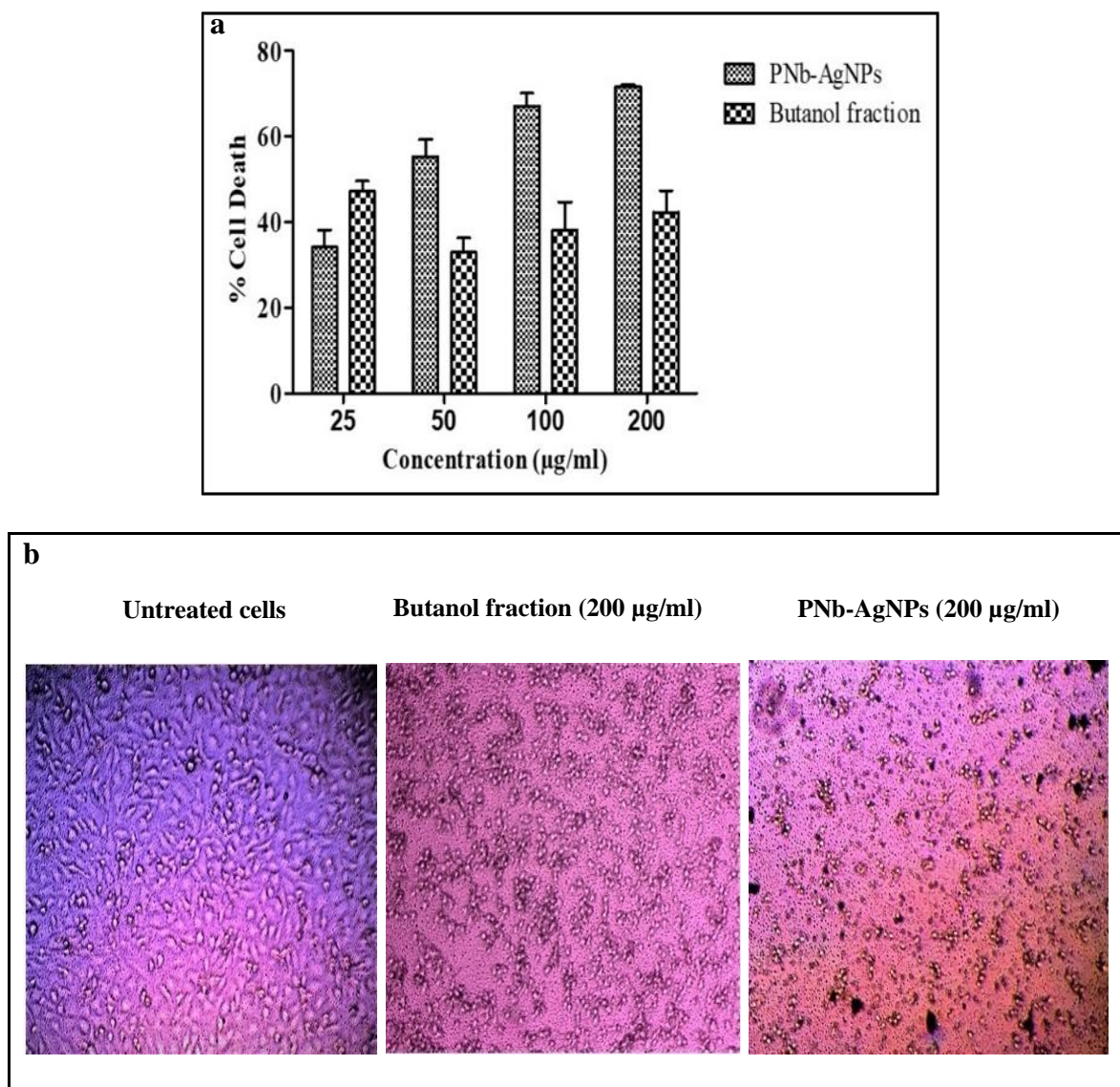


Figure 1. (a) Cytotoxicity of PNb-AgNPs against EAC cells at various concentrations after 24 h of incubation (b) Morphological observations (20 \times magnification) of untreated EAC cells, cells treated with butanol fraction (200 $\mu\text{g/ml}$) of *P. roxburghii* and PNb-AgNPs (200 $\mu\text{g/ml}$).

Moreover, PNb-AgNPs also displayed non-toxic effects on normal human breast cells (fR2) and peripheral blood lymphocytes [16]. Previously, anticancer potential of biosynthesized silver nanoparticles against various cancer cells like MCF-7 (human breast cancer cells), HT-29, HCT-116 (Human Colon Cancer Cells), and A549 (lung carcinoma) [25-28] and their non-toxic behavior towards normal cells have been reported [29]. This data

depicted that PNb-AgNPs have promising anticancer potential without any toxicity towards normal cells.

3.2. Determination of intracellular ROS generation.

It has been shown earlier that ROS generation activates apoptotic signal transduction pathways [30]. PNb-AgNPs (200 $\mu\text{g/ml}$) treated EAC cells showed a four-fold increase in the ROS levels, compared to that of the control. There was negligible ROS production in EAC cells treated with butanol fraction of *P. roxburghii* compared to the untreated cells (Figure 2a). According to the previous studies, one of the feasible anticancer mechanisms of action of AgNPs could be the production of ROS and oxidative stress that damages cell integrity, leading to apoptotic cell death [31]. It has been reported that an increase in cell viability was observed after the addition of a ROS scavenger, which specifies ROS to be a predominant mechanism in AgNPs cytotoxicity [32]. Thus, these results suggest that the enhanced anticancer efficiency of PNb-AgNPs might be due to elevated levels of ROS in EAC cells.

3.3. PNb-AgNPs induces loss of MMP.

Loss of mitochondrial function is a significant determinant and indicator of cell death, which can be assessed by monitoring changes in MMP [33, 34]. The results showed a decrease in MMP (68.6 %) of EAC cells when treated with PNb-AgNPs, whereas in butanol fraction treated cells, a 37.2 % reduction in MMP was recorded. The data depict that PNb-AgNPs induces mitochondrial depolarization in EAC cells that may lead to apoptosis (Figure 2b). Previous studies have reported that increased ROS production leads to the formation of mitochondrial permeability transition pores, which activates mitochondria-dependent apoptotic pathways.

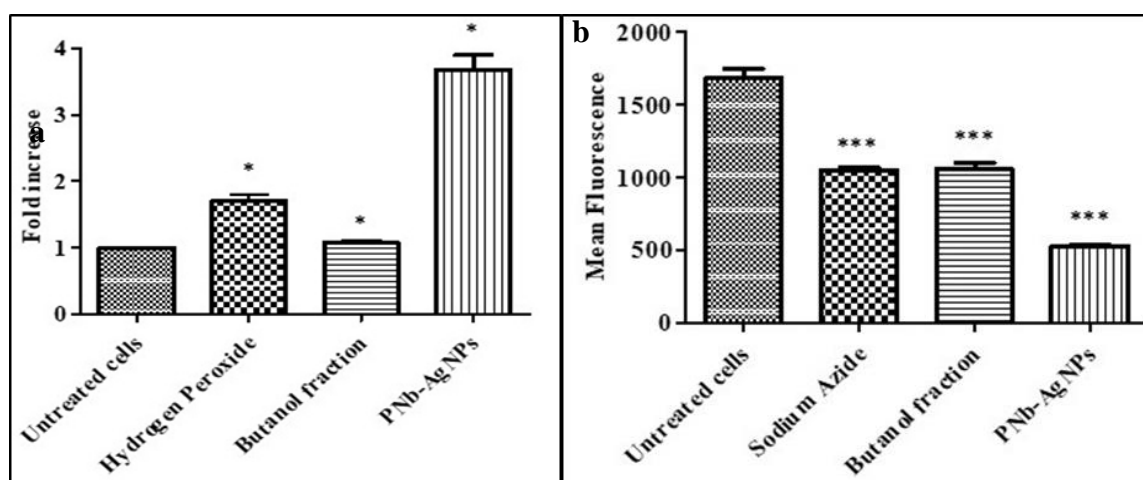


Figure 2. (a) Intracellular ROS generation; (b) mitochondrial potential analysis EAC cells after 30 min treatment with butanol fraction of *P. roxburghii* and PNb-AgNPs (200 $\mu\text{g/ml}$). Results were expressed as mean \pm SEM of three different experiments. Data is significant showing * $p < 0.05$; *** $p < 0.001$. H_2O_2 (100 μM) and sodium azide were used as positive controls in these experiments, respectively.

The mitochondrial depolarization has been shown as a primary mechanism of AgNPs induced cytotoxicity, which also involves crosstalk between the mitochondria and other cellular components [35]. The present study suggests that ROS generation and mitochondrial depolarization by PNb-AgNPs initiates apoptosis in EAC cells.

3.4. Cell cycle analysis.

The distribution of PNB-AgNPs treated EAC cells in various cell cycle phases was examined by flow cytometry. The cell cycle is a complex process where cells receive different growth-controlling signals integrated and processed at various points known as checkpoints [36, 37]. EAC cells exposed to PNB-AgNPs (200 µg/ml) for 24 h displayed an increase in the sub-G1 phase cells (52 %) as compared to butanol fraction (200 µg/ml) treated and doxorubicin (positive control, 50 µg/ml) treated cells (43% and 22%, respectively) (Figure 3). The apoptotic cells which have DNA fragmentation show a typical sub-G1 peak in DNA histogram [38]. The increased number of cells in the sub-G1 phase of PNB-AgNPs treated cells indicate the DNA damage and apoptosis in EAC cells.

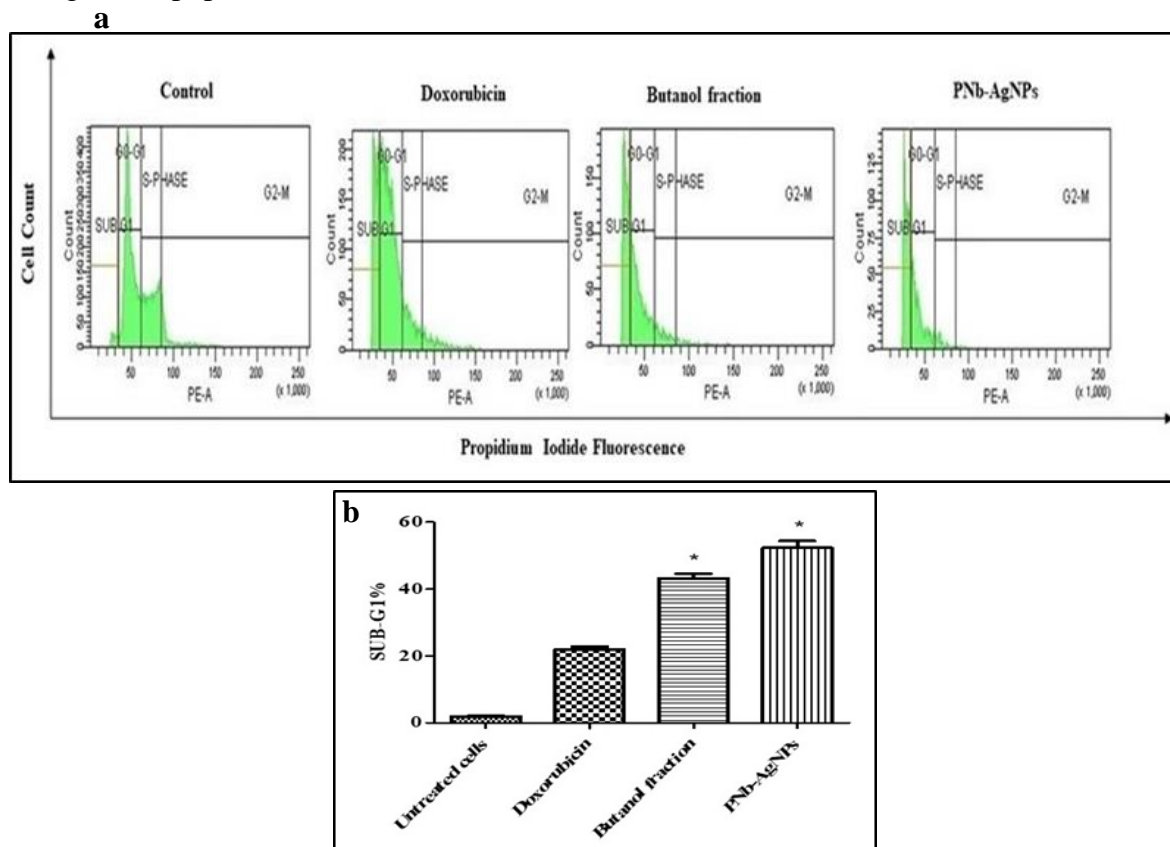


Figure 3. (a) Effect of butanol fraction of *P. roxburghii* and PNB-AgNPs after 24 h treatment on cell cycle progression; (b) The graph shows % of cells present in the sub-G1 phase. Data is significant with * $p < 0.05$.

3.5. Nuclear morphology and DNA fragmentation.

The apoptotic nuclear morphology was analyzed after treating EAC cells with PNB-AgNPs for 24 hours. As shown in Figure 4a, the untreated cells displayed normal nuclei (smooth nucleus), whereas PNB-AgNPs treated cells showed condensation and fragmentation of the nucleus that are hallmarks of apoptosis [39]. In butanol fraction treated and doxorubicin treated EAC cells, a very faint fragmented nucleus was observed after 24 hours of incubation (Figure 4a).

Fragmentation of genomic DNA is an important feature for intrinsic apoptotic cell death. DNA fragmentation usually results in a characteristic ladder, which is visualized by agarose gel electrophoresis [40]. As shown in Figure 4b (lane 5), PNB-AgNPs (200 µg/ml) treated EAC cells displayed a unique ladder-like DNA fragmentation pattern after 24 hours of incubation while in butanol fraction (200 µg/ml) treated and doxorubicin treated EAC cells,

very little DNA fragmentation was observed. (Figure 4b, lanes 3 and 4). The results confirmed that PNb-AgNPs induced DNA damage, thereby leading to apoptosis in EAC cells. Taken together, PNb-AgNPs can act as novel cancer therapeutics that can induce apoptosis in EAC cells via mitochondrial disruption, ROS generation, cell cycle perturbation, and finally, DNA destruction.

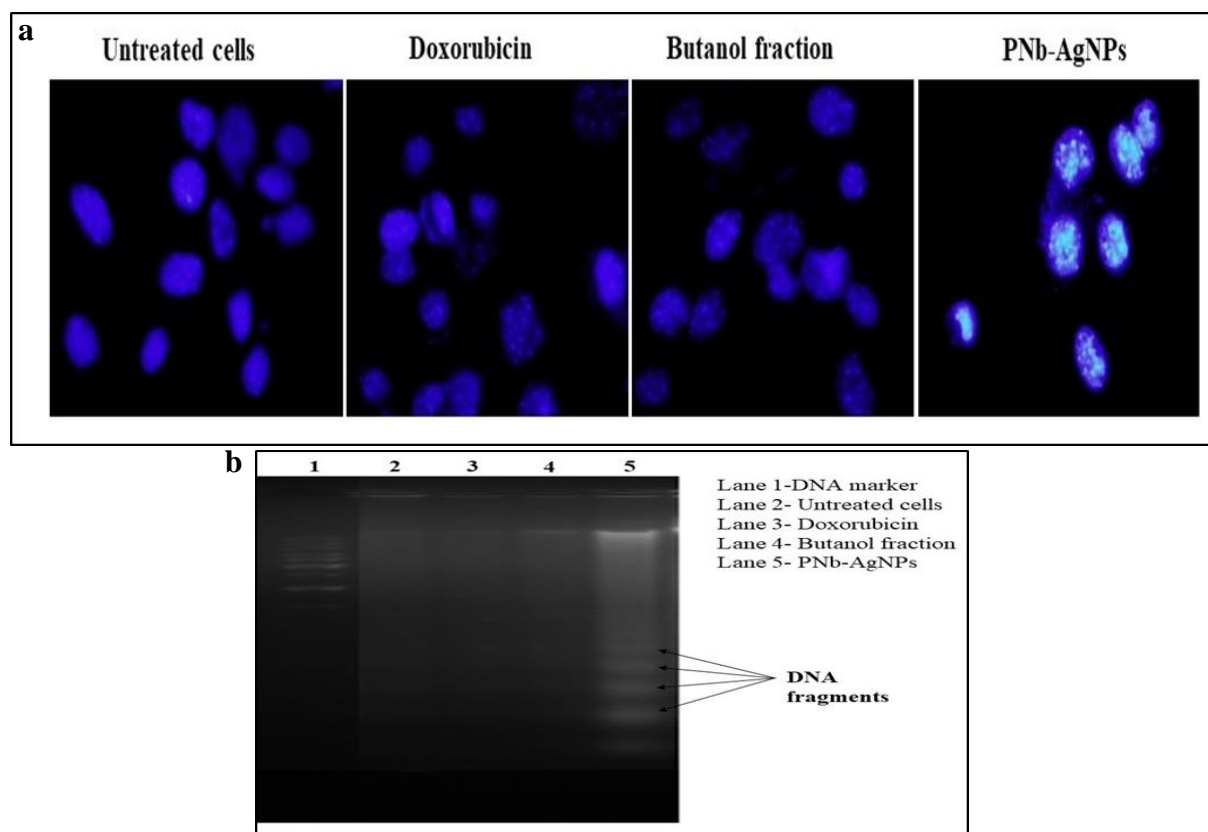


Figure 4. (a) Fluorescent microscopic images of EAC cells following treatment with PNb-AgNPs and butanol fraction of *P. roxburghii* (200 µg/ml); (b) Effect of PNb-AgNPs on DNA fragmentation. The fragmented DNA is shown by arrows with solid lines.

3.6. Toxicological measurement by hemolytic assay.

The most crucial aspect of any drug is that it should be biocompatible, i.e., it should be non-toxic towards healthy cells. As described above, the PNb-AgNPs are non-toxic to normal epithelial cells. All the substances that enter the circulatory system come in contact with RBC [41]. Here, the RBC lysis assay analyzed the biocompatibility of the synthesized PNb-AgNPs and butanol fraction of *P. roxburghii*. Different concentrations (125, 250, 500, 1000 µg/ml) of butanol fraction and PNb-AgNPs were exposed to RBCs, and data showed that butanol fraction causes negligible RBC lysis. PNb-AgNPs showed 3.77 ± 0.07 % RBC lysis at a concentration of 1000 µg/ml (Table 1). Since < 5% hemolysis is permissible for biocompatibility of any drug [42], PNb-AgNPs can be considered as biocompatible and non-toxic to healthy cells even at 1000 µg/ml, being safe to use as drugs or drug carrier systems for biomedical applications.

Table 1. Hemolytic analysis after exposure to butanol fraction and PNb-AgNPs at various concentrations for 1 h. Results were presented as mean \pm SEM and the experiments were done in triplicate.

Sample	Concentration (µg/ml)	Hemolysis %
Phosphate Buffer Saline (PBS)		0.02 ± 0.02 (negative control)
Triton X- 100		100 ± 4.31 (positive control)

Sample	Concentration (µg/ml)	Hemolysis %
Butanol fraction	125	0.17 ± 0.08
	250	0.29 ± 0.17
	500	0.35 ± 0.04
	1000	0.58 ± 0.12
PNb-AgNPs	125	1.43 ± 0.22
	250	2.90 ± 0.03
	500	3.06 ± 0.08
	1000	3.77 ± 0.08

3.7. In vivo anticancer studies.

3.7.1. Effect of PNb-AgNPs on body weight, tumor size, and tumor volume.

Anticancer activity of PNb-AgNPs was evaluated against EAC-bearing Swiss albino mice. In the ascites tumor model, butanol fraction of *P. roxburghii* and PNb-AgNPs (6 mg/kg body wt. and 2 mg/kg body wt., respectively) were administered intraperitoneally for 14 days, and body weight was measured each day. The bodyweight of the tumor-bearing mice was found to increase significantly from day 0 to day 14.

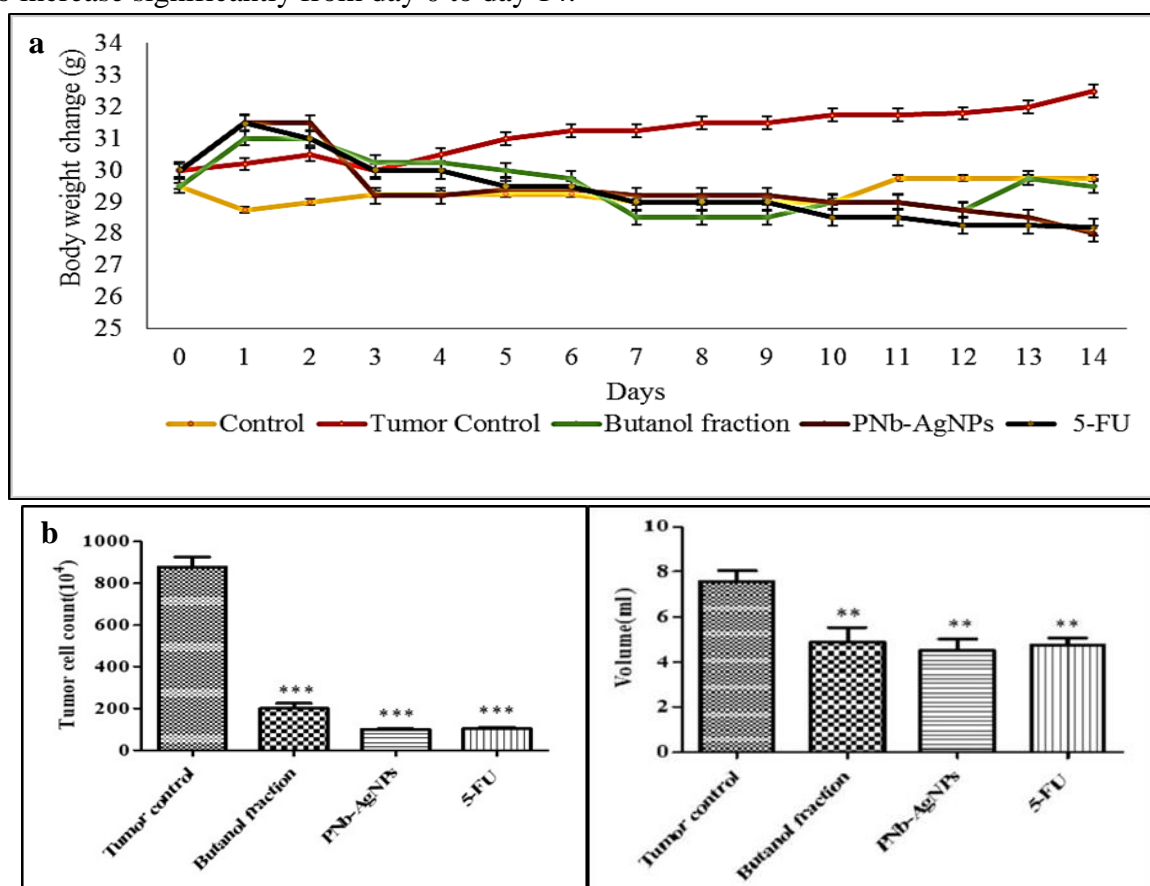


Figure 5. (a) Effect of butanol fraction of *P. roxburghii* and PNb-AgNPs on body weight of EAC bearing tumor mice; (b) EAC cells withdrawn from the peritoneal cavity of tumor control and treated groups were counted; (c) Tumor volume was measured by the volume of ascites fluid withdrawn from the peritoneal cavity. Data is statistically significant with * $p < 0.05$, ** $p < 0.01$, *** $p < 0.001$ when compared with control.

A significant reduction in the body weight was observed in the EAC bearing mice treated with PNb-AgNPs, butanol fraction, and 5-FU (Figure 5a). This reduction in body weight is directly associated with the total cell count in ascites fluid and peritoneal fluid volume, which serve as a direct nutritional source to the tumor cells [43]. On the 14th day, 877

$\times 10^4$ EAC cells were counted in peritoneal fluid of untreated mice (Group II), whereas butanol fraction and PNb-AgNPs treated groups have 200×10^4 and 99×10^4 EAC cells, respectively (77 % and 88.6 % tumor growth inhibition, Figure 5b).

Similarly, 5-FU treated mice group has 104×10^4 cells depicting 88 % tumor growth inhibition. Additionally, the volume of ascetic fluid was significantly reduced in the EAC-bearing mouse treated with butanol fraction, PNb-AgNPs, and 5-FU compared to the untreated tumor-bearing mice group (Figure 5c). It has previously been shown that phycocyanin fabricated AgNPs significantly inhibited the tumor cell volume, tumor cells count, and tumor weight in EAC-bearing mice [44]. The results indicate that PNb-AgNPs can inhibit the tumor growth induced by EAC cells in the experimental animals.

3.7.2. Hematological changes.

The results showed that the hemoglobin content and RBC count (11.35 ± 0.85 g/dl and 7.14 ± 0.50 /mm³, respectively) were found to reduce in tumor-bearing mice as compared to the normal group (13.85 ± 0.15 g/dl and 8.94 ± 0.21 /mm³, respectively). PNb-AgNPs, butanol fraction of *P. roxburghii*, and 5-FU treated mice showed restoration of hemoglobin content and RBC count as that of the control group, as shown in Table 2. Moreover, the WBC count was also found to be enhanced in EAC bearing mice group (9.25 ± 0.05 /mm³) compared to the normal group (6.00 ± 0.20 /mm³). In the mice treated with PNb-AgNPs and 5-FU, WBC count (7.35 ± 0.15 /mm³ and 7.60 ± 0.30 /mm³, respectively) was a little higher as compared to the normal group (Table 2) but lower than EAC bearing mice suggesting that PNb-AgNPs treatment reduced the WBC level to reach the normal level. However, the WBC count in the group treated with butanol fraction was lower than (4.20 ± 0.10 /mm³) that of untreated normal mice (Group I). The restoration of hemoglobin content, RBC, and WBC count suggest that PNb-AgNPs possess hematopoietic protective action [45-47].

3.7.3. Biochemical changes.

The level of liver enzymes (AST, ALT, and ALP) in EAC tumor-bearing mice was substantially higher than normal mice (Group II vs. Group I, Table 2).

Table 2. Analysis of hematological and biochemical parameters of normal control group mice (Group I), tumor control (Group II), butanol fraction treated (Group III), PNb-AgNPs treated (Group IV), and 5-FU (Group V) treated EAC bearing mice.

	Group I	Group II	Group III	Group IV	Group V
Hematological parameters					
Hemoglobin (g/dl)	13.85 ± 0.15	11.35 ± 0.85	13.00 ± 0.70	13.35 ± 0.35	13.15 ± 0.85
RBC (Cells cu.mm)	8.94 ± 0.21	7.14 ± 0.50	9.02 ± 0.17	9.43 ± 0.43	8.30 ± 0.24
WBC (Cells cu.mm)	6.00 ± 0.20	9.25 ± 0.05	4.20 ± 0.10	7.35 ± 0.15	7.60 ± 0.30
Biochemical parameters					
AST (IU/l)	153 ± 3.50	249 ± 3.50	192 ± 2.00	157 ± 2.50	161 ± 1.00
ALT (IU/l)	29 ± 1.00	99 ± 2.00	63 ± 3.50	40 ± 1.50	36 ± 1.00
ALP (IU/l)	78 ± 2.00	260 ± 2.50	150 ± 1.50	161 ± 2.50	154 ± 1.50

Whereas in PNb-AgNPs and 5-FU treated mice, the liver enzymes' activity was found to be reduced compared to the EAC bearing mice (Table 2). An increase in the liver function parameters (AST, ALT, and ALP) occurs because of impaired liver functions in tumor-bearing mice [48]. Restoration of these parameters as normal values after treatment with butanol fraction and PNb-AgNPs treatments (Group III and Group IV) indicated that this

nanoformulation of *P. roxburghii* phyto-contents along with silver is capable of maintaining normal liver functions in EAC bearing mice.

3.7.4. Histopathological analysis.

Histopathology of the liver tissue samples was performed to determine any adverse effects of the butanol fraction of *P. roxburghii* and PNb-AgNPs on tumor-bearing mice (Figure 6). The data showed that the group I mice have normal liver cells, and there were two foci of lymphocytes, one along a central vein and the other in the left field. The group II tumor-bearing mice displayed scattered, larger and darker nuclei (hyperchromatic) in liver cells suggesting degeneration of these cells with mild excess of Kupffer cells in sinusoids. Bialy *et al.* observed similar hepatic morphological changes in EAC-bearing mice [49]. Mice treated with butanol fraction (Group III), PNb-AgNPs (Group IV), and 5-FU (Group V) exhibited no toxicity to liver tissues. Liver section images were comparable to that of Group I normal mice. Nagarajan *et al.* have shown earlier that cotton plant-mediated AgNPs are non-toxic to mice organs [50].

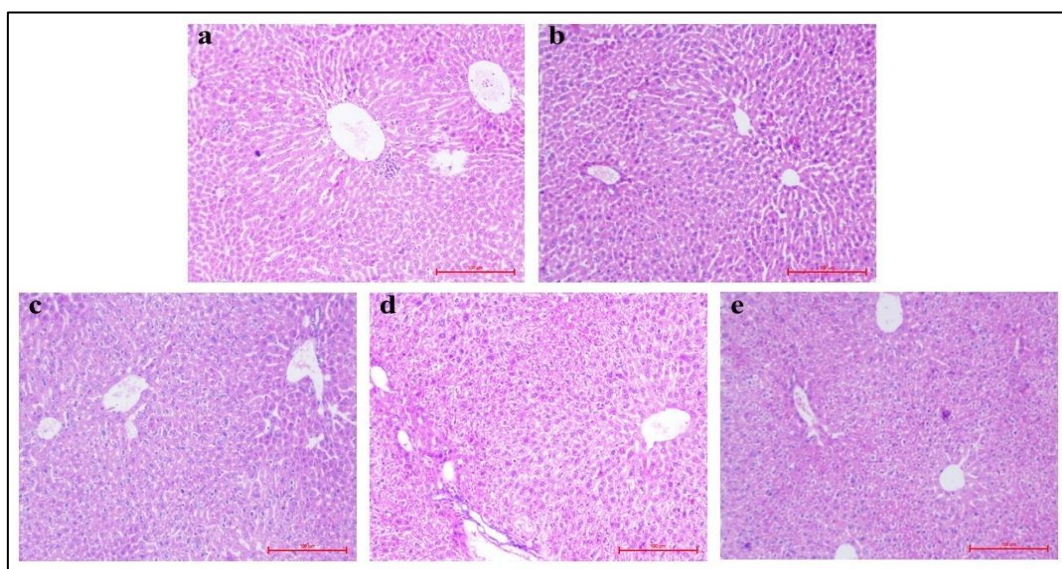


Figure 6. Histopathological examination of liver in control and treated mice, the liver section of (a) Group I normal mice with no abnormality; (b) Group II; EAC induced mice; (c) Group III; EAC induced mice treated with butanol fraction (6 mg/Kg body wt.); (d) Group IV; EAC induced mice treated with PNb-AgNPs (2 mg/Kg body wt.); (e) Group V; mice treated with 20 mg/Kg body wt. 5-FU (H&E, scale bar 100 μ m, magnification 100 \times).

4. Conclusions

The current study showed that PNb-AgNPs exhibited significant anticancer potential both under *in vitro* and *in vivo* conditions. Under *in vitro* conditions, PNb-AgNPs treatment increased the ROS levels, mitochondrial membrane depolarization, and DNA damage leading to cancer cell death. Nuclear morphology alterations and an increase in the sub-G1 population also display apoptosis induction mediated through these non-toxic and biocompatible silver nanoparticles. Additionally, the *in vivo* study also revealed that PNb-AgNPs could inhibit EAC growth in female Swiss Albino mice without affecting hematological parameters and liver function. In conclusion, the combination of *P. roxburghii* components and silver at a nano-level could be a potential anticancer agent.

Funding

The authors are thankful to the Centre of Research on Himalayan Sustainability and Development, Shoolini University of Biotechnology and Management Sciences (SURF/CRSHT/2016-020), for providing facilities and financial support.

Acknowledgment

The authors would like to acknowledge Maharishi Markandeshwar (Deemed to be University) for the support.

Conflicts of Interest

The authors declare no conflict of interest.

References

1. Plackal Adimuriyil George, B.; Kumar, N.; Abrahamse, H.; Ray, S.S. Apoptotic efficacy of multifaceted biosynthesized silver nanoparticles on human adenocarcinoma cells. *Sci. Rep.* **2018**, *8*, 14368, <https://doi.org/10.1038/s41598-018-32480-5>.
2. Bray, F.; Ferlay, J.; Soerjomataram, I.; Siegel, R.L.; Torre, L.A.; Jemal, A. Global cancer statistics 2018: GLOBOCAN estimates of incidence and mortality worldwide for 36 cancers in 185 countries. *CA Cancer J. Clin.* **2018**, *68*, 394-424, <https://doi.org/10.3322/caac.21492>.
3. Aslan, B.; Ozpolat, B.; Sood, A.K.; Lopez-Berestein, G. Nanotechnology in cancer therapy. *J. Drug Targeting* **2013**, *21*, 904-913, <https://doi.org/10.3109/1061186X.2013.837469>.
4. Chidambaram, M.; Manavalan, R.; Kathiresan, K. Nanotherapeutics to Overcome Conventional Cancer Chemotherapy Limitations. *Journal of Pharmacy & amp; Pharmaceutical Sciences* **2011**, *14*, 67-77, <https://doi.org/10.18433/J30C7D>.
5. Mani, S.; Balasubramanian, M.G.; Ponnusamy, P.; Vijayan, P. Antineoplastic Effect of PAC Capped Silver Nanoparticles Promote Apoptosis in HT-29 Human Colon Cancer Cells. *J. Cluster Sci.* **2019**, *30*, 483-493, <https://doi.org/10.1007/s10876-019-01510-1>.
6. Vivek, K.C.; Anshuman, S.; Vinay, K.S.; Mohan, P.S. Cancer Nanotechnology: A New Revolution for Cancer Diagnosis and Therapy. *Curr. Drug Metab.* **2019**, *20*, 416-429, <https://doi.org/10.2174/1389200219666180918111528>.
7. Indu, H.; Reena, V.S.; Reena, K.; Prashant, K.; Utkrishta, L.R. Inspection and Remedy of Cervical Cancer Using Nanoparticles. *Nanoscience & Nanotechnology-Asia* **2018**, *8*, 186-192, <https://doi.org/10.2174/2210681207666170323155831>.
8. Buttacavoli, M.; Albanese, N.N.; Cara, G.D.; Alduina, R.; Faleri, C.; Gallo, M.; Pizzolanti, G.; Gallo, G.; Feo, S.; Baldi, F.; Cancemi, P. Anticancer activity of biogenerated silver nanoparticles: an integrated proteomic investigation. *Oncotarget* **2017**, *9*, <https://doi.org/10.18632/oncotarget.23859>.
9. Pathania, D.; Sharma, G.; Kumar, A. *Modified Biopolymers*; Nova Science Publishers, Incorporated, **2017**.
10. Hira, I.; Kumar, A.; Kumari, R.; Saini, A.K.; Saini, R.V. Pectin-guar gum-zinc oxide nanocomposite enhances human lymphocytes cytotoxicity towards lung and breast carcinomas. *Materials and Engineering: C* **2018**, *90*, 494-503, <https://doi.org/10.1016/j.msec.2018.04.085>.
11. Iravani, S.; Zolfaghari, B. Green Synthesis of Silver Nanoparticles Using Pinus eldarica Bark Extract. *BioMed Research International* **2013**, *2013*, 639725, <https://doi.org/10.1155/2013/639725>.
12. Sharma, M.; Monika; Thakur, P.; Saini, R.V.; Kumar, R.; Torino, E. Unveiling antimicrobial and anticancerous behavior of AuNPs and AgNPs moderated by rhizome extracts of Curcuma longa from diverse altitudes of Himalaya. *Sci Rep.* **2020**, *10*, 10934, <https://doi.org/10.1038/s41598-020-67673-4>.
13. Pfeffer, C.M.; Singh, A.T.K. Apoptosis: a target for anticancer therapy. *Int. J. Mol. Sci.* **2018**, *19*, 448, <https://doi.org/10.3390/ijms19020448>.
14. Zhu, B.; Li, Y.; Lin, Z.; Zhao, M.; Xu, T.; Wang, C.; Deng, N. Silver Nanoparticles Induce HePG-2 Cells Apoptosis Through ROS-Mediated Signaling Pathways. *Nanoscale Research Letters* **2016**, *11*, 198, <https://doi.org/10.1186/s11671-016-1419-4>.

15. Vaid, P.; Raizada, P.; Saini, A.K.; Saini, R.V. Biogenic silver, gold and copper nanoparticles - A sustainable green chemistry approach for cancer therapy. *Sustainable Chemistry and Pharmacy* **2020**, *16*, 100247, <https://doi.org/10.1016/j.scp.2020.100247>.
16. Kumari, R.; Saini, A.K.; Kumar, A.; Saini, R.V. Apoptosis induction in lung and prostate cancer cells through silver nanoparticles synthesized from *Pinus roxburghii* bioactive fraction. *Journal of Biological Inorganic Chemistry* **2020**, *25*, 23-37, <https://doi.org/10.1007/s00775-019-01729-3>.
17. Ceylan, D.; Aksoy, A.; Ertekin, T.; Yay, A.H.; Nisari, M.; Karatoprak, G.Ş.; Ülger, H. The effects of gilaburu (*Viburnum opulus*) juice on experimentally induced Ehrlich ascites tumor in mice. *J. Cancer Res. Ther.* **2018**, *14*, 314.
18. Abdel-Gawad, E.I.; Hassan, A.I.; Awwad, S.A. Efficiency of calcium phosphate composite nanoparticles in targeting Ehrlich carcinoma cells transplanted in mice. *Journal of Advanced Research* **2016**, *7*, 143-154, <https://doi.org/10.1016/j.jare.2015.04.001>.
19. Ozaslan, M.; Karagoz, I.D.; Kilic, I.H.; Guldur, M.E. Ehrlich ascites carcinoma. *African Journal of Biotechnology* **2011**, *10*, 2375-2378.
20. Zhao, J.; Riediker, M. Detecting the oxidative reactivity of nanoparticles: a new protocol for reducing artifacts. *J. Nanopart. Res.* **2014**, *16*, 2493, <https://doi.org/10.1007/s11051-014-2493-0>.
21. Baracca, A.; Sgarbi, G.; Solaini, G.; Lenaz, G. Rhodamine 123 as a probe of mitochondrial membrane potential: evaluation of proton flux through F₀ during ATP synthesis. *Biochim. Biophys. Acta* **2003**, *1606*, 137-146, [https://doi.org/10.1016/S0005-2728\(03\)00110-5](https://doi.org/10.1016/S0005-2728(03)00110-5).
22. Giri, K.; Ghosh, U.; Bhattacharyya, N.P.; Basak, S. Caspase 8 mediated apoptotic cell death induced by β -sheet forming polyalanine peptides. *FEBS Lett.* **2003**, *555*, 380-384, [https://doi.org/10.1016/S0014-5793\(03\)01294-8](https://doi.org/10.1016/S0014-5793(03)01294-8).
23. Parthiban, E.; Manivannan, N.; Ramanibai, R.; Mathivanan, N. Green synthesis of silver-nanoparticles from *Annona reticulata* leaves aqueous extract and its mosquito larvicidal and anti-microbial activity on human pathogens. *Biotechnology Reports* **2019**, *21*, e00297, <https://doi.org/10.1016/j.btre.2018.e00297>.
24. Ratan, Z.A.; Haidere, M.F.; Nurunnabi, M.; Shahriar, S.M.; Ahammad, A.J.; Shim, Y.Y.; Reaney, M.J.T.; Cho, J.Y. Green Chemistry Synthesis of Silver Nanoparticles and Their Potential Anticancer Effects. *Cancers (Basel)* **2020**, *12*, 855, <https://doi.org/10.3390/cancers12040855>.
25. Jang, S.J.; Yang, I.J.; Tettey, C.O.; Kim, K.M.; Shin, H.M. In-vitro anticancer activity of green synthesized silver nanoparticles on MCF-7 human breast cancer cells. *Materials Science and Engineering: C* **2016**, *68*, 430-435, <https://doi.org/10.1016/j.msec.2016.03.101>.
26. Priyadharshini, R.I.; Prasannaraj, G.; Geetha, N.; Venkatachalam, P. Microwave-Mediated Extracellular Synthesis of Metallic Silver and Zinc Oxide Nanoparticles Using Macro-Algae (*Gracilaria edulis*) Extracts and Its Anticancer Activity Against Human PC3 Cell Lines. *Appl. Biochem. Biotechnol.* **2014**, *174*, 2777-2790, <https://doi.org/10.1007/s12010-014-1225-3>.
27. Hamouda, R.A.; Hussein, M.H.; Abo-elmagd, R.A.; Bawazir, S.S. Synthesis and biological characterization of silver nanoparticles derived from the cyanobacterium *Oscillatoria limnetica*. *Sci. Rep.* **2019**, *9*, 13071, <https://doi.org/10.1038/s41598-019-49444-y>.
28. Pei, J.; Fu, B.; Jiang, L.; Sun, T. Biosynthesis, characterization, and anticancer effect of plant-mediated silver nanoparticles using *Coptis chinensis*. *International journal of nanomedicine* **2019**, *14*, 1969-1978, <https://doi.org/10.2147/IJN.S188235>.
29. Bagur, H.; Poojari, C.C.; Melappa, G.; Rangappa, R.; Chandrasekhar, N.; Somu, P. Biogenically Synthesized Silver Nanoparticles Using Endophyte Fungal Extract of *Ocimum tenuiflorum* and Evaluation of Biomedical Properties. *J. Cluster Sci.* **2020**, *31*, 1241-1255, <https://doi.org/10.1007/s10876-019-01731-4>.
30. Zhang, J.; Wang, X.; Vikash, V.; Ye, Q.; Wu, D.; Liu, Y.; Dong, W. ROS and ROS-Mediated Cellular Signaling. *Oxid. Med. Cell. Longev.* **2016**, *2016*, 4350965, <http://dx.doi.org/10.1155/2016/4350965>.
31. Bhatnagar, S.; Kobori, T.; Ganesh, D.; Ogawa, K.; Aoyagi, H. Biosynthesis of silver nanoparticles mediated by extracellular pigment from *Talaromyces purpurogenus* and their biomedical applications. *Nanomaterials* **2019**, *9*, 1042, <https://doi.org/10.3390/nano9071042>.
32. Chahal, A.; Saini, A.K.; Chhillar, A.K.; Saini, R.V. Natural antioxidants as defense system against cancer. *Asian J Pharm Clin Res* **2018**, *11*, 38-44, <https://doi.org/10.22159/ajpcr.2018.v11i5.24119>.
33. Giampazolias, E.; Tait, S.W.G. Mitochondria and the hallmarks of cancer. *The FEBS Journal* **2016**, *283*, 803-814, <https://doi.org/10.1111/febs.13603>.

34. Hwang, I.-s.; Lee, J.; Hwang, J.H.; Kim, K.-J.; Lee, D.G. Silver nanoparticles induce apoptotic cell death in *Candida albicans* through the increase of hydroxyl radicals. *The FEBS Journal* **2012**, *279*, 1327-1338, <https://doi.org/10.1111/j.1742-4658.2012.08527.x>.
35. Gurunathan, S.; Qasim, M.; Park, C.; Yoo, H.; Kim, J.-H.; Hong, K. Cytotoxic potential and molecular pathway analysis of silver nanoparticles in human colon cancer cells HCT116. *Int. J. Mol. Sci.* **2018**, *19*, 2269, <https://doi.org/10.3390/ijms19082269>.
36. Rhind, N.; Russell, P. Signaling pathways that regulate cell division. *Cold Spring Harb. Perspect. Biol.* **2012**, *4*, a005942, <https://doi.org/10.1101/cshperspect.a005942>.
37. Langerak, P.; Russell, P. Regulatory networks integrating cell cycle control with DNA damage checkpoints and double-strand break repair. *Philosophical Transactions of the Royal Society B: Biological Sciences* **2011**, *366*, 3562-3571, <https://doi.org/10.1098/rstb.2011.0070>.
38. Kajstura, M.; Halicka, H.D.; Pryjma, J.; Darzynkiewicz, Z. Discontinuous fragmentation of nuclear DNA during apoptosis revealed by discrete “sub-G1” peaks on DNA content histograms. *Cytometry Part A* **2007**, *71A*, 125-131, <https://doi.org/10.1002/cyto.a.20357>.
39. Afsar, T.; Trembley, J.H.; Salomon, C.E.; Razak, S.; Khan, M.R.; Ahmed, K. Growth inhibition and apoptosis in cancer cells induced by polyphenolic compounds of *Acacia hydaspica*: Involvement of multiple signal transduction pathways. *Sci. Rep.* **2016**, *6*, 23077, <https://doi.org/10.1038/srep23077>.
40. Gurunathan, S.; Han, J.W.; Eppakayala, V.; Jeyaraj, M.; Kim, J.-H. Cytotoxicity of Biologically Synthesized Silver Nanoparticles in MDA-MB-231 Human Breast Cancer Cells. *BioMed Research International* **2013**, *2013*, 535796, <https://doi.org/10.1155/2013/535796>.
41. Huang, H.; Lai, W.; Cui, M.; Liang, L.; Lin, Y.; Fang, Q.; Liu, Y.; Xie, L. An Evaluation of Blood Compatibility of Silver Nanoparticles. *Sci. Rep.* **2016**, *6*, 25518, <https://doi.org/10.1038/srep25518>.
42. Choi, J.; Reipa, V.; Hitchins, V.M.; Goering, P.L.; Malinauskas, R.A. Physicochemical Characterization and In Vitro Hemolysis Evaluation of Silver Nanoparticles. *Toxicol. Sci.* **2011**, *123*, 133-143, <https://doi.org/10.1093/toxsci/kfr149>.
43. Salem, M.L.; Shoukry, N.M.; Teleb, W.K.; Abdel-Daim, M.M.; Abdel-Rahman, M.A. In vitro and in vivo antitumor effects of the Egyptian scorpion *Androctonus amoreuxi* venom in an Ehrlich ascites tumor model. *SpringerPlus* **2016**, *5*, 570, <https://doi.org/10.1186/s40064-016-2269-3>.
44. El-Naggar, N.E.-A.; Hussein, M.H.; El-Sawah, A.A. Bio-fabrication of silver nanoparticles by phycocyanin, characterization, in vitro anticancer activity against breast cancer cell line and in vivo cytotoxicity. *Sci. Rep.* **2017**, *7*, 10844, <https://doi.org/10.1038/s41598-017-11121-3>.
45. Avula, M.; Somasekhar, A.; Sumanjali, A.; Kumar, B.; Prasanna, B.; Vali, T.; Bhargavi, D. Anticancer activity of *Tephrosia purpurea* root extracts against Ehrlich Ascites Carcinoma (EAC) cells in swiss albino mice. *Der Pharmacia Sinica* **2014**, *5*, 81-87.
46. Kathiriya, A.; Das, K.; Kumar, E.P.; Mathai, K.B. Evaluation of antitumor and antioxidant activity of *Oxalis corniculata* Linn. against Ehrlich ascites carcinoma on mice. *International Journal of Cancer Management* **2010**, *4*, 157-165.
47. Antony, J.J.; Sithika, M.A.A.; Joseph, T.A.; Suriyakalaa, U.; Sankarganesh, A.; Siva, D.; Kalaiselvi, S.; Achiraman, S. In vivo antitumor activity of biosynthesized silver nanoparticles using *Ficus religiosa* as a nanofactory in DAL induced mice model. *Colloids Surf. B. Biointerfaces* **2013**, *108*, 185-190, <https://doi.org/10.1016/j.colsurfb.2013.02.041>.
48. Suresh Kumar, R.B.; Kar, B.; Dolai, N.; Karmakar, I.; Bhattacharya, S.; Haldar, P.K. Antitumor activity and antioxidant status of *Streblus asper* bark against Dalton's ascitic lymphoma in mice. *Interdiscip. Toxicol.* **2015**, *8*, 125-130, <https://doi.org/10.1515/intox-2015-0019>.
49. El Bialy, B.E.; Hamouda, R.A.; Khalifa, K.S.; Hamza, H.A. Cytotoxic effect of biosynthesized silver nanoparticles on Ehrlich ascites tumor cells in mice. *International Journal of Pharmacology* **2017**, *13*, 134-144, <https://doi.org/10.3923/ijp.2017.134.144>.
50. Kanipandian, N.; Li, D.; Kannan, S. Induction of intrinsic apoptotic signaling pathway in A549 lung cancer cells using silver nanoparticles from *Gossypium hirsutum* and evaluation of in vivo toxicity. *Biotechnology Reports* **2019**, *23*, e00339, <https://doi.org/10.1016/j.btre.2019.e00339>.